A Comprehensive Study of Thermo-Physical Properties of Investment Shells

Mingzhi Xu
Missouri University of Science and Technology

ABSTRACT

Investment shell molds are typically built up with metastable amorphous silica binder and may include fused (amorphous) silica flour as filler and crushed fused silica grains as stucco. These metastable amorphous (non-crystalline) materials can crystallize (devitrify) at elevated temperature during industrial process and the amount of transformed amorphous phase depends on temperature, time at temperature, and the presence of mineralizers. The degree to which these amorphous phase materials devitrify during the process will affect the thermo-mechanical properties, which controls the solidification and ceramic shell integrity. In this article, influences of firing temperature on the thermo-mechanical properties of silica-based shell molds were investigated. The thermal properties were also correlated to the degree of phase transformations, which can occur during sequential heating/cooling cycles in investment casting processing.

Keywords: investment shell, firing temperature, phase transformation, thermal property, mechanical property

INTRODUCTION

Investment shell molds have been widely used to produce near-net shape castings, especially with complex geometry and thin sections[1-6]. Process simulation of the investment casting is often used in modern foundry practice because it is able to predict and eliminate many types of casting defects, such as shrinkage, porosity, and hot tears. Accurate representation of the thermal properties of the ceramic shell is critically important for realistic simulation of casting solidification.
Many researchers have attempted to accurately determine the thermal properties of shell molds utilizing different methods. Numerous equations have been proposed since 1939 to account the effect of porosity on thermal conductivity[7-13]. However, those equations worked only for certain materials or types of porosity within a very limited temperature range.

Several experimental and simulation methods have been developed to determine the thermal properties of the highly porous investment shell mold material. The hot wire method was used to measure the thermal conductivity of industrial shell materials[14-16]. However, the hot wire method assumes that the material is isotropic in all radial directions and thus is not well applicable to investment shells[17]. The layered structure in investment shells requires a more directional measurement technique.

A laser flash method for directional measurements of thermal diffusivity and specific heat capacity was first introduced by Shinzato and Baba[18-19]. This method uses thin (1-3 mm thickness) specimens and could be applicable for measuring the properties of thin layers. Using this technique, Connolly[20] and Konrad[21] have measured the thermal properties of investment casting shells up to 1300°C. More recently, Sabau[17]pointed out that the laser flash method had low accuracy when measuring the thermal properties for investment casting shells. It was found that a thin fused silica shell specimen had a suitable thermal response time during measurement but the results could be affected by the unimpeded laser light penetration through the shell due to large voids in the structure. On the other hand, thick fused silica shell specimen could not be used since it does not have a suitable response time during the measurements. Also, the open pores on the specimen surface variably reduce the actual thickness of the specimen which creates significant uncertainties in the measurement. Garcia et al.[22] presented a method to solve this problem by attaching two thin copper disks to a porous specimen to ensure a known effective thickness and eliminate the penetration of the laser. However this method is not applicable for a brittle investment ceramic shell. Xu et al.[23-24] utilized a three dimensional optical profiler to determine the effective thickness of the specimen and improved the accuracy of laser flash method for measuring thermal properties of a specimen with porous surfaces.

The inverse method is another way to estimate the “real-time” thermal properties of the entire shell during casting solidification. The inverse method is based on matching the real cooling curves obtained from the casting and the

shell during the process to the computer simulated cooling curves by varying the properties of interest[23-28]. In this method, the thermal properties measured from the laser flash method were used as the starting point for the inverse simulations. A well-established starting point near the final value is beneficial to get the best agreement with the physics from the optimization used for the inverse method. In the inverse simulations of unsteady state heat transfer in the casting/shell/environment system, some well-defined thermal properties are also used as the input to help calculate the unknown properties.

The thermal properties obtained from the inverse method are considered as the realistic properties for simulation purpose. However, the laser flash method can be treated as an ideal method for measurement of near steady state thermal properties because a thin specimen is thermally equilibrated before taking measurement. The laser flash method is suitable for capturing property changes due to process changes at fixed test temperature. This test facilitates understanding of the mechanism of property changes by relating the properties to specific temperatures.

It is reasonable to expect that the shell processing thermal history is an important factor, in addition to ceramic composition, which influences the investment shell thermo-physical properties. Generally, a shell mold, constituting a mixture of a set of thermodynamically metastable ceramic ingredients, is exposed in several thermal cycles before the final casting is poured. These thermal cycles may include (i) drying and aging of wet mold (ii) heating for pattern removal, (iii) sintering during firing, (iv) an additional reheating before pouring and, finally, (v) heating/cooling cycle during pouring liquid metal, casting solidification, and cooling. Considering that the colloidal silica binder as well as the flour filler and most stucco ceramics are amorphous to a significant extent, the degree to which the amorphous to crystalline transformation takes place during the processing also has a great effect on the thermal properties of ceramic shell[29-31].

It is implied by the procedures of industrial practices that the thermal history has great direct and indirect effects on investment shell properties and casting quality; however, only restricted studies have been done to quantify these effects. Mahimkar et al.[30] measured the heat capacity of different shell systems exposed to different thermal histories and these authors drew a correlation between the change of the heat capacity and the silica phase transformations. Meulenberg et al.[31] detected the phase transformation of silica binder from being completely amorphous in the unfired condition to cristobalite within the usual firing temperature range between 900°C and 1500°C, in which range zircon remains stable.

In this study, influences of firing temperature on the thermal and mechanical properties of silica-based shell molds were investigated. The thermal properties were also correlated to the degree of phase transformations, which can occur during sequential heating/cooling cycles in investment casting processing.

EXPERIMENTAL

SHELL BUILDING

Expanded Polystyrene (EPS) foam pattern was used in this study. Colloidal silica binder, -200 mesh fused silica flour and 30/50 mesh fused silica stucco were used to build shells. The slurry consists of 33 wt. % of silica binder and 67 wt. % of silica flour. The slurry was mixed for 24 hours to achieve constancy. The viscosity of the slurry was tested using a Brookfield DV-II+ Pro viscometer equipped with a LV3 spindle operating at 30rpm. The dynamic slurry viscosity was maintained at 1100±100cP for the prime coat and 600±50cP for the back-up and seal coats.

The foam patterns were lightly abraded using a 1200-grit sandpaper to remove surface texture differences between cut and uncut surfaces. The patterns were submerged in the slurry for twenty seconds. Then the patterns were removed and excess slurry was allowed to naturally drip off for one minute. During drip removal, patterns were rotated around the vertical axis at a speed of 10rpm with the dipped end facing down and oriented at a 45° angle from the vertical axis. Stucco was then applied onto the slurry coat in a rainfall sander. A uniform distribution of stucco was achieved by turning the samples at a constant speed until no additional stucco would adhere to the wet surface. The samples were allowed to air dry for at least four hours before the next layer was applied. For each sample, one prime coat, five back-up coats and one seal coat were applied.

PATTERN REMOVAL AND SHELL FIRING

After being dried for minimum one additional day in a controlled humidity room, the foam pattern was carefully burned out by a propane torch under a hood. Then the shells were put into a cold laboratory chamber furnace and heated up at a rate of 30ºC/min to different firing temperature individually (600°C (1112°F), 850°C (1562°F) or 1000°C (1832°F)), then held for one hour prior to testing. The shells were allowed to cool down in the chamber overnight. They were subsequently tested at temperatures of 200°C, 400°C, 600°C, 800°C, 1000°C and 1200°C by laser flash and X-ray diffraction using the temperature cycle shown in Figure 1A. The composition of each layer of the shell is given in Table 1.

DEVELOPED LASER FLASH METHOD

Laser flash was used to determine the specific heat capacity and the thermal conductivity of the shells. A graphite disk was used as the reference material. The specimens were machined to 12.7 *mm* by 12.7 *mm* by about 2 *mm* thick disks. To insure similar emissivity, the front and rear faces of both the reference and the test specimens were covered with a sprayed graphite coating. Surface roughness due to porosity in the specimen was measured by a 3-D optical profiler.

Table 1. Composition of the silica based investment shell.

Coat (Number of layers)	**Slurry**	**Fused silica stucco particle size, mm**
Prime coat (one)	Colloidal silica (1-100 *nm*) + fused silica flour (2-20 μm) (1:2 by weight). Viscosity 1100cP±100cP	0.3-0.6
Backup coats (five)	Colloidal silica (1-100 *nm*) + fused silica flour (2-20 μm) (1:2 by weight). Viscosity 600cP±100cP	0.3-0.6
Seal coat (one)	Colloidal silica (1-100 *nm*) + fused silica flour (2-20 μm) (1:2 by weight). Viscosity 600cP±100cP	N/A

The effective thickness of each specimen was determined based on total thickness and the surface roughness adjustment. The effective thickness was used to calculate thermal properties[19, 23-24]. The samples were placed into a cold furnace and heated to 1200°C (2192°F) at a heating rate of 15°C/min (27°F/min) then cooled to room temperature at 30°C/min (54°F/min). During the thermal cycle, laser flash was performed at every 200°C (360°F) from 200°C (392°F) to 1200°C (2192°F) upon heating and cooling, after the samples were held for 10 minutes at each elevated temperature (Figure 1a).

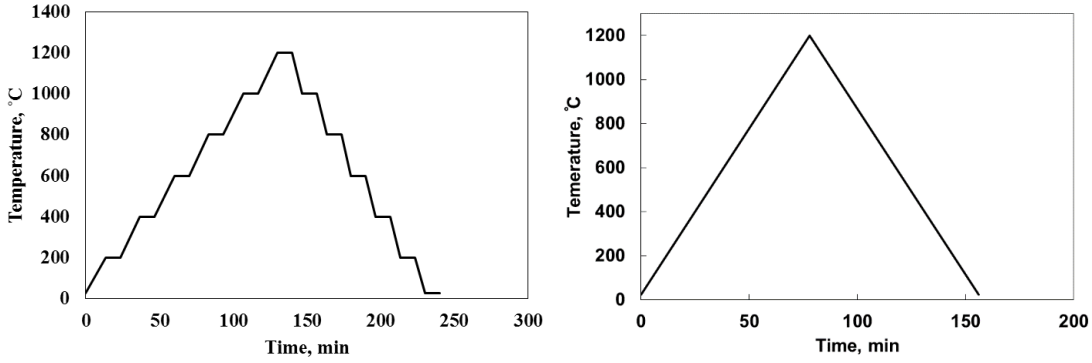

(a) (b)

Figure 1. The temperature regime used for high temperature tests: (a) X-ray diffraction and laser flash method, 15 ℃/min (27°F/min) heating and 30 ℃/min (54°F/min) cooling rates, with a 10 min hold at each elevated temperature; (b) DTA, 15 ℃/min (27°F/min) continuous heating and cooling rates

HIGH TEMPERATURE X-RAY DIFFRACTION

X-ray diffraction (XRD) was performed using a diffractometer. The shells were finely powdered to minus 100 mesh and loaded on a platinum strip (Pt diffraction peaks were shown in Figure 2). The specimens were heated in the chamber at a 15°C/min (27°F/min) heating rate up to 1200°C (2192°F) then cooled to 25°C (77°F) with a 30°C/min (54°F/min) cooling rate. During the heating and cooling process, the specimens were held for 10 minutes at temperature from 200°C (392°F) to 1200°C (2192°F) with an interval of 200°C (360°F) (Figure 1a). At the end of each hold, XRD data were collected in a step 2θ-scan mode from 10° to 70° with a total counting time of five minutes, using an incident wavelength of 1.54 Å. A scan was also performed at room temperature before and after the thermal cycle.

DIFFERENTIAL THERMAL ANALYSIS

Differential thermal analysis (DTA) was performed. Before testing, the samples were dried at 110°C (230°F) for 1 hour. High purity Al_2O_3 powder was used as the reference material. Experiments were performed under air atmosphere at a flow rate of 50 mL/min. Samples were heated from room temperature to 1200°C (2192°F) at a heating rate of 15°C/min (27°F/min) and then cooled to room temperature at the same rate (Figure 1b).

SPECIFIC SURFACE AREA.

Brunauer–Emmett–Teller (BET) method was used to determine the specific surface area of the shell samples. Colloidal silica binder was dehydrated and hand crushed using a mortar and pestle to a certain size for which the equivalent spherical surface area would be orders of magnitude below the measured value of the BET method. The crushed silica binder was fired at different temperatures, 600°C (1112°F), 850°C (1562°F) and 1000°C (1832°F), for 1 hour. Afterwards, the powder was well blended and dehydrated at 120°C (248°F) for another 2 hours before the test. The specific surface area in m^2 per gram of powder was measured at the temperature of liquid nitrogen.

DENSITY AND POROSITY.

The bulk density and open porosity accessible to water of the shells were measured using Archimedes method[32]. The same specimen were then crushed and the true density was measured by a *He*-Pycnometer, in which all of the pores were filled by *He* and the true volume of the powder can be measured.

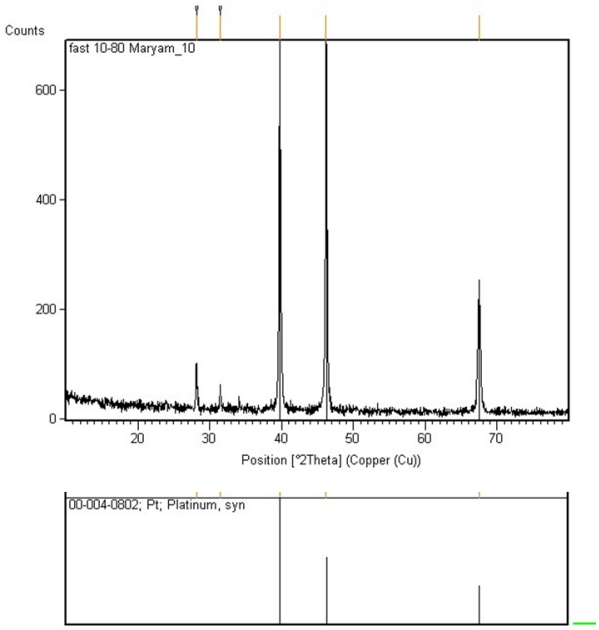

Figure 2. X-ray diffraction pattern of a reference platinum strip at room temperature showing some spurious indications at 2θ of 28°, 31°and 34°which were excluded from subsequent measurements

THREE-POINT FLEXURAL TEST.
Moduli of Rupture (MoR) of the shells were measured according to ASTM C1161[33] using a three point bend test apparatus at room temperature after the shells were fired at the elevated temperatures for one hour.

RESULTS

DENSITIES AND POROSITIES
Table 2 shows the densities and porosities of shells under different firing conditions. Measurements were made at room temperature after firing the shells at different temperatures. These results indicate that the firing process decreases closed and total porosities. It is found that a higher firing temperature results lower closed and total porosity values due to a higher degree of sintering.

Table 2. Room temperature density and porosity of shells fired at different temperatures

Pre-firing temperature, ˚C (˚F)	**Bulk density, g/cm^3**	**True density, g/cm^3**	**Open porosity accessible to water, %**	**Closed porosity, %**	**Total porosity, %**
Unfired (green)	1.77±0.04	2.64±0.03	16.2±0.2	16.6±2.1	32.8±1.9
600 (1112°F)	1.73±0.03	2.55±0.02	18.4±0.1	13.8±1.5	32.1±1.4
850 (1562°F)	1.83±0.02	2.60±0.01	17.1±0.1	12.4±0.9	29.5±0.8
1000 (1832°F)	1.76±0.02	2.42±0.01	16.8±0.1	10.7±0.8	27.5±0.7

EFFECT OF FIRING TEMPERATURE ON SHELL THERMAL PROPERTIES.
The specific heat capacity (C_p) and the coefficient of thermal conductivity (K) of the shells subjected to different firing temperatures were measured by the developed laser flash method. The properties of shells upon heating and cooling during the measurements are plotted in Figure 3. In all of the shells, both C_p

and *K* values increase with increasing test temperature. During the heating, the thermal conductivity of the three shells are similar, while the shell fired at 850°C (1562°F) has a decreased thermal conductivity during the cooling cycle. Differences on the heat capacity among these three shells were noticed after the shells were heated to 1200°C (2192°F). These discrepancies in C_p and *K* values indicate a certain amount of devitrification happens during this particular test thermal cycle, which can have an effect on the thermal properties.

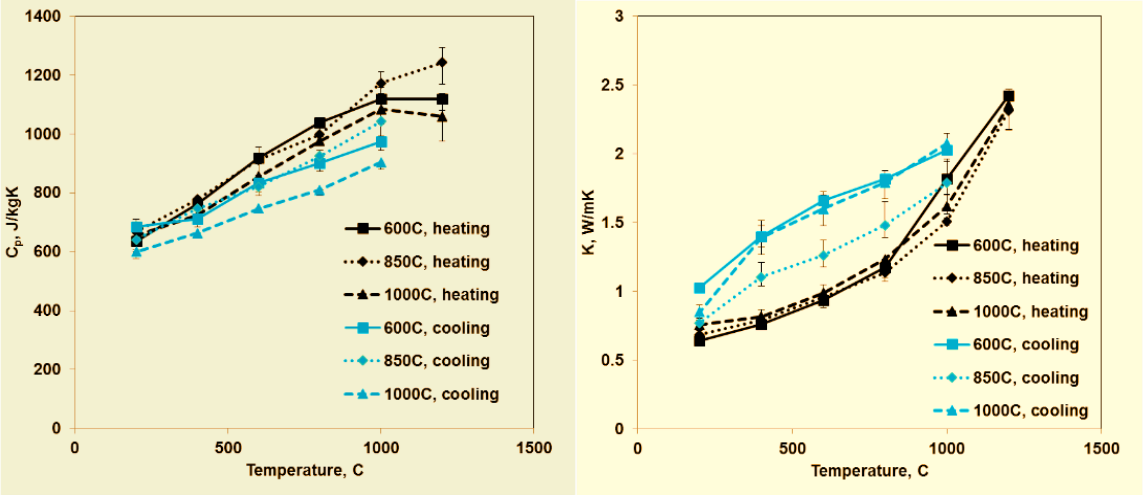

(a) (b)

Figure 3. Heat capacity (a) and thermal conductivity (b) of fired shells measured from the laser flash method; firing temperature and thermal cycles are indicated in the legends

EFFECT OF FIRING TEMPERATURE ON SHELL MECHANICAL PROPERTIES.

Room temperature three-point bend test results (Figure 4) show that after firing the shell at 600°C (1112°F), there isn't any significant sintering, thus the modulus of rupture (MoR) of the shell doesn't have a noticeable change, compared to the green shell. However, the MoR of the shell increases at relatively higher firing temperatures, 850°C (1562°F) and 1000°C (1832°F), due to an extended amount of sintering. Nevertheless, at an even higher firing temperature of 1200°C (2192°F), the MoR decreases significantly. This can be the result of the devitrification where the difference in volume changes introduces more defects as the shells cool down after being fired.

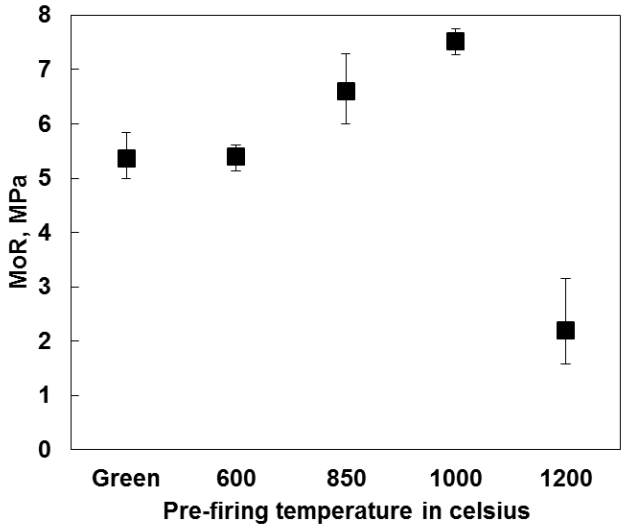

Figure 4. Modulus of Rupture (MoR) of silica shell molds fired at different temperature; tests were performed at room temperature

SILICA BINDER DEVITRIFICATION TEMPERATURE.

To identify the components of the shell which are predominant with respect to the phase transformation, high temperature XRD tests were performed individually on each of the components used for investment shells, including silica binder, fused silica flour, and fused silica stucco. Devitrification was only found in the silica binder at temperatures above 1000°C (1832°F), while the other components remained amorphous during the test up to1200°C (2192°F) (Figure 5a). This is because silica binder has a much smaller particle size (1-100 nm) than the other components (2 µm – 0.6 mm). Thus silica binder has a higher surface area to volume ratio which could provide an additional activation energy component as well as an easy transport path for transformation. The DTA results (Figure 5b) also indicate that the silica binder starts devitrification at around 1000°C (1832°F). These data are supported by a study[29] which also found that amorphous silica transformed to cristobalite at 1000°C (1832°F).

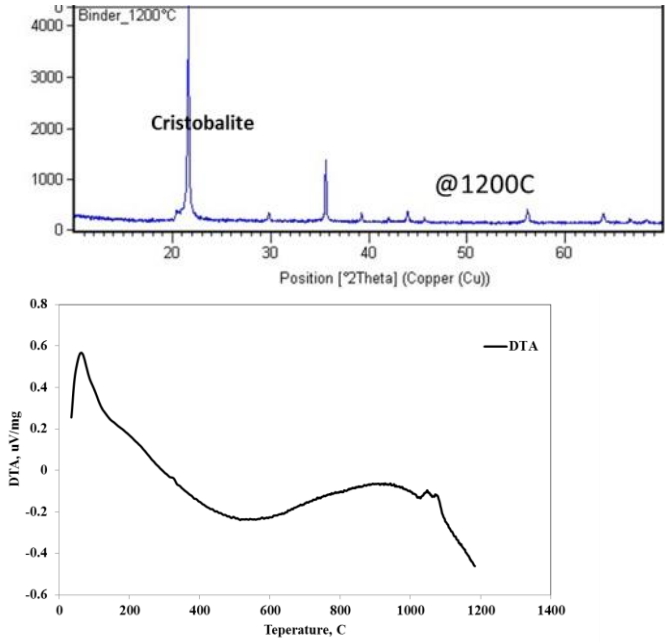

(a) (b)

Figure 5. XRD at 1200°C (2192°F) shows the presence of cristobalite (a) and DTA test shows the devitrification temperature is around 1020°C (1868°F) (b)

PHASE TRANSFORMATION DURING FIRING AND PRE-HEATING.

According to a typical investment casting process sequence used in many high production volume investment casting foundries, the shells are fired after pattern removal, cooled down, and inspected. Then shellsare subjected to a second short pre-heating, just before pouring. Last pre-heating stage is necessary to minimize the heat loss during pouring, allowing liquid metal to fill the narrow cavities of the hot mold. These multiple heating/cooling cycles will affect the solid phase transformations in the shell.

<u>After firing cycle</u>

Phases that are present in the shells after the firing cycles were studied by XRD. In this case, XRD tests were performed at room temperature on the shells fired at different temperatures. It is found (Figure 6) that the shell fired at 1000°C (1832°F) has a crystalline peak, while other shells (green and fired at lower temperatures) have just amorphous phase. In the case of a multi-component shell, at a firing temperature of 1000°C (1832°F), phase transformation in silica binder starts and the cristobalite may nucleate at the boundary with silica flour, however the

silica stucco is inert. The broad crystalline peak in Figure 6(d) indicates that most of the crystallites have a very small grain size.

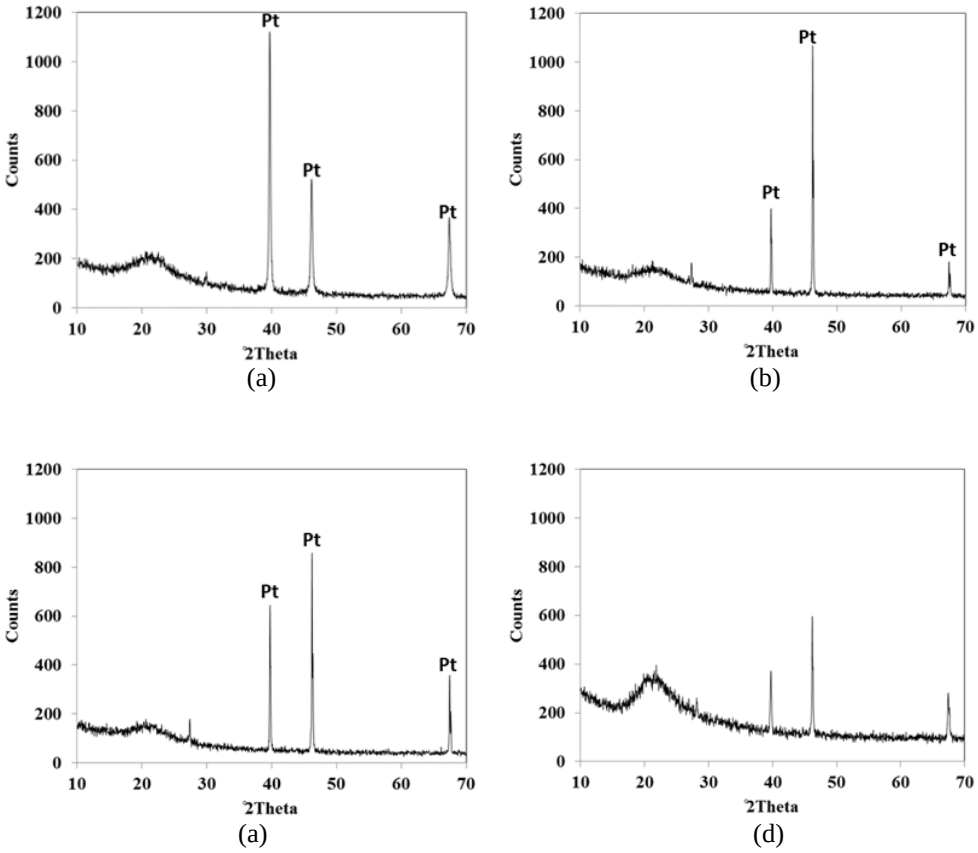

Figure 6. Room temperature XRD patterns of ceramic shell fired at different temperatures: (a) green, not fired, (b) 600°C (1112°F), (c) 850°C (1562°F), and (d) 1000°C (1832°F)

Dynamic phase transformation during reheating

After the shells are fired, the shells were reheated up to 1200°C (2192°F) and XRD tests were performed at 1200°C (2192°F). As shown in Figure 7, the green shell and shell previously fired at a low temperature (600°C or 1112°F) have a very sharp peak of cristobalite, while the shell previously fired at 850°C (1562°F) and reheated after that doesn't have much of phase transformation. In the shell fired at 1000°C (1832°F), the cristobalite, which has already formed during the firing process, grows to larger particle sizes during the subsequent 1200°C (2192°F) reheating cycle.

Specific Surface Area Change during Firing and Reheating

During firing and reheating, sintering as well as devitrification could occur simultaneously in the shell. The amount of sintering can be represented by the direct measurements of the specific surface area change on the silica binder. The specific surface area was measured after the silica binder was fired at different temperatures. Measurements were repeated after the fired binder was reheated to 1200°C (2192°F) and held for one hour.

As shown in Figure 8, after firing shells at different temperatures, the binder fired at 600°C (1112°F) does not exhibit significant change in the specific surface area, which indicates that a minimum amount of coarsening takes place at this temperature. When the binder was fired at 850°C (1562°F), a small reduction (20%) in specific surface area is observed and this could be the result of vitreous sintering without devitrification. A dramatic decrease in

specific surface area (from 53 m^2/g to 0.1 m^2/g), after firing the colloidal silica binder at 1000°C (1832°F), shows a significant extent of sintering.
When the fired colloidal silica binder is reheated to 1200°C (2192°F), it is found that the surface areas of all of the colloidal silica binders are reduced to the similar level, indicating that firing temperature doesn't have a big effect on the sintering when the binders are subjected to a higher reheating temperature.

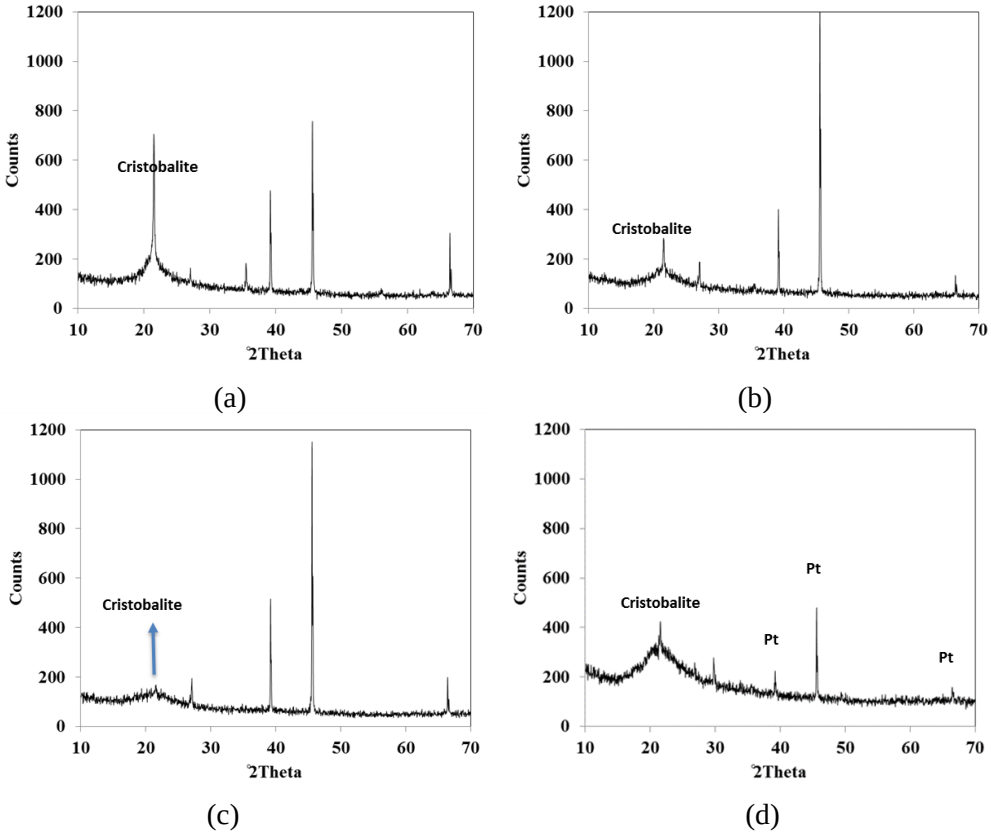

Figure 7. XRD patterns at 1200°C of the shells which are reheated to 1200°C after different thermal processing: ***green condition (a), preliminary fired at 600°C (b), 850°C (c), and 1000°C (d)***

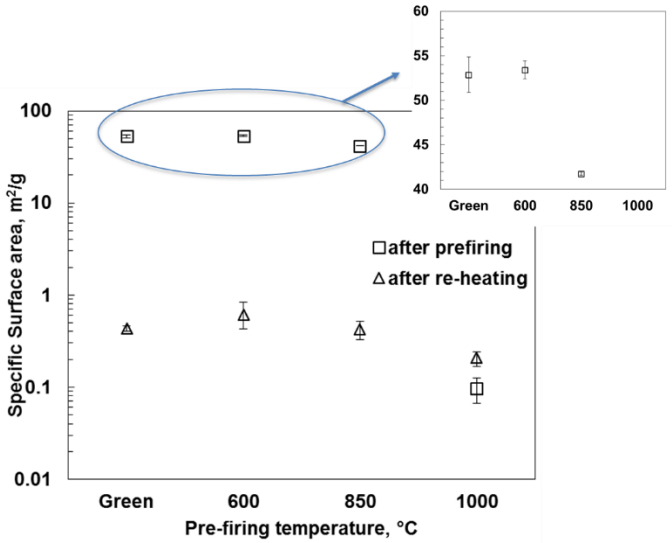

Figure 8. Specific surface area of the colloidal silica binder after being fired at different temperatures; measurements were repeated after the fired binder samples were reheated to 1200°C (2192°F) and held for one hour

DISCUSSION

EFFECT OF FIRING TEMPERATURE ON SPECIFIC SURFACE AREA AND PHASE TRANSFORMATION
DTA results (Figure 5b) show that silica binder is the only constituent that devitrifies at 1000°C (1832°F). Thus when firing the shell at 1000°C (1832°F), it is just enough to start the devitrification kinetically, but at a rather slow rate. Thus only small crystalline sizes of cristobalite is found from the XRD tests (Figure 6d). The coarsening was still predominant during firing at this temperature, thus a dramatic specific surface area loss is noticed (Figure 8). Thermodynamic software FactSage 6.4 was used to calculate the Gibbs free energy change (ΔG) of one mole of silica from amorphous to cristobalite (h) at 1200°C (2192°F): ΔG = -2500J. Taking the surface energy of amorphous silica as 0.26 J/m^2 [34], the surface energy stored in one mole of amorphous silica binder decreases by almost 1000J when surface area is reduced from 53m^2/g (green state) to 0.1 m^2/g (fired at 1000°C or 1832°F). This suggests that surface energy could provide a significant component of the activation energy for the devitrification reactions. Additionally, this surface area lost will impede the reaction rate for the phase transformation since a higher surface area provides a more favorable reaction path. Consequently when reheating the shells (previously fired at 1000^0 C or 1832°F) to 1200°C (2192°F) after firing, less amorphous silica devitrifies than in a shell fired at lower temperatures. However the cristobalite previously formed during firing could grow to a larger grain size due to grain growth, which is consistent with a sharper cristobalite peak being observed in XRD (Figure 7d). Similarly, when firing the shell at 850°C (1562°F), the specific surface area decreases by more than 20% (Figure 8) due to sintering, and less devitrification takes place when that shell is reheated to 1200°C (2192°F) than would occur in shells fired at a lower temperature. The shell fired at 600°C (1112°F) doesn't have any significant sintering thus retains similar specific surface area compared to the green shell. When reheating shell fired at 600°C and the green shell, sharp cristobalite peaks were obtained on the diffraction patterns.

In summary, a higher firing temperature, in the temperature range below the amorphous silica devitrification temperature, decreases the reactivity of the binder towards devitrification or the rate of devitrification.

EFFECT OF FIRING TEMPERATURE ON THERMAL PROPERTIES.
The atomic-scale disorder present in the amorphous silica causes its thermal conductivity to be lower than the conductivity of the cristobalite, because the structural disorder impedes the motion of the mobile photon thus lowering the thermal conductivity. When correlating the XRD results with the thermal properties measured by the laser flash method, it is noticed that the shell fired at 600°C (1112°F) has the greatest amount of cristobalite formation, subsequently the highest thermal conductivity. The shell which has been fired at 850°C (1562°F) exhibits a very limited amount of cristobalite formation and shows a lower thermal conductivity. The shell fired at 1000°C (1832°F) not only has some amount of devitrification during the firing process, but when being reheated to 1200°C (2192°F), the already formed cristobalite grows to larger grain sizes. This eliminates some grain boundaries that impede the photon movement, thus higher thermal conductivity values are expected.
In the case of specific heat capacity, the shell fired at 850°C (1562°F) doesn't devitrify as much as the shells fired at 600°C (1112°F) and 1000°C (1832°F), thus the heat capacity values increase with increasing temperature within the temperature range from 200°C to 1200°C (2192°F), similar to the behavior of amorphous silica. However, the shell fired at 600°C (1112°F) devitrifies at above 1000°C (1832°F) during the laser flash measurements. The transformation from amorphous silica to cristobalite is an exothermic reaction. The heat generated in this transformation is 9500 J/mole or 158 J/g. In other words, assuming the heat capacity of silica at 1 J/gK, this energy is enough to increase the temperature of one gram silica by over 150°C (270°F).
In the differential laser flash calorimetry method, a reference specimen (subscript "R") and the test specimen (subscript "M"), are mounted together under the same condition at the same temperature and irradiated uniformly with homogenized laser beam. The temperature rise (ΔT) of the reference (graphite) with known specific heat capacity (C_p) and the temperature rise of the test specimen are both measured with non-contact infrared radiation thermometer. If the density (ρ) and thickness (L) are known, then the specific heat capacity of the specimen can be calculated (Eqn.1):

$$\left(\rho c_p\right)_M = \frac{L_R \Delta T_R}{L_M \Delta T_M}\left(\rho c_p\right)_R \qquad \text{Eqn. 1}$$

Due to the abrupt temperature rise resulted by the phase transformation, it will cause an overestimate of the temperature rise in Equation 1. Consequently, a decreased heat capacity value is calculated at 1200°C (2192°F). This exothermic phase transformation effect correlates to the laser flash measurements (Figure 3a) very well.

EFFECT OF FIRING TEMPERATURE ON MECHANICAL PROPERTIES

A relatively higher firing temperature within the range studied,850°C (1562°F) and 1000°C (1832°F), provides more significant sintering and as a result, the MoR of the shell increases. However, as shown in Figure 4, when firing shells at an even higher temperature of 1200°C (2192°F), the MoR of the shell significantly decreases. According to the DTA results shown in Figure 5b, the devitrification range for amorphous silica starts at 1020°C (1868°F). When firing the shells at 1000°C (1832°F), the sintering effect is still predominate on increasing the shell strength. However, when increasing the firing temperature to 1200°C (2192°F), a significant amount of cristobalite was formed in the shell. During cooling, the volume change of cristobalite, as it passes through the low-temperature inversion range, is reported to be 7%[35]. These volume changes could result more micro-cracking, weakening the structure (Figure 9).

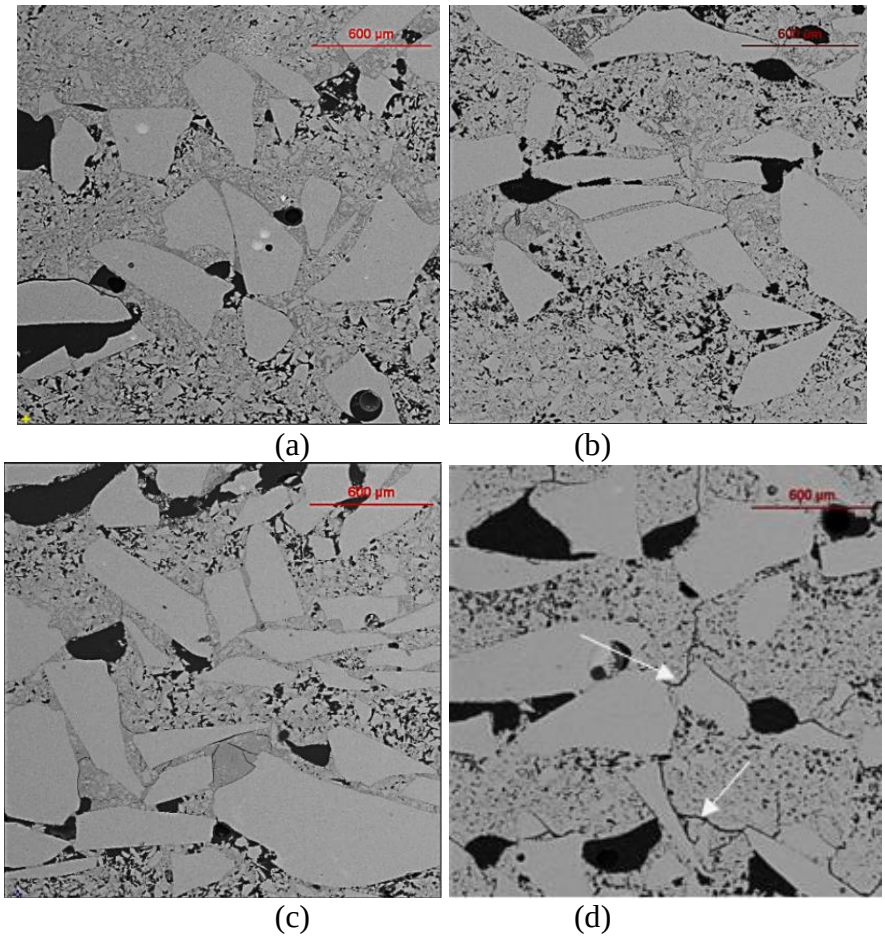

(a) (b)

(c) (d)

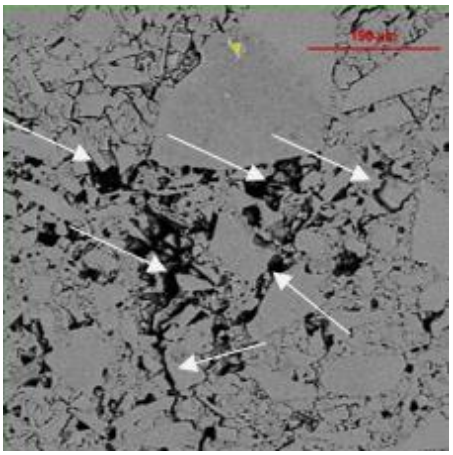

(e)

Figure 9. Microstructure of silica shells after being fired at different temperatures: green (a), 600°C (1112°F) (b), 850°C (1562°F) (c), 1000°C (1832°F) (d), 1200°C (2192°F) (e) showing that a high firing temperature of 1200°C (2192°F) causes more micro-cracking when the shells are cooled down due to the difference in volume change resulted by devitrification

Moreover, a higher firing temperature results in more coarsening, thus larger grain sizes are expected in the bond phase of a shell fired at 1200°C (2192°F). Spontaneous cracking occurs predominately in large-grained samples because the reduction in the internal strain energy is proportional to the cube of the particle size whereas the increased surface energy caused by the fracture is proportional to the square of the particle size[36]. These energy differentials or differences mean that large-grain samples above a critical size are weak and in general have poor physical properties because of the substantial grain/matrix interface stresses. Consequently grain coarsening in the bond phase may contribute to the crack propagation.

APPLICATION

This research initiated quantitative study of amorphous silica devitrification in investment shells. More firing profiles need to be studied to complete this work. However, based on the current results, one can see that the firing profiles significantly affects the thermos-physical properties of the shells. In an investment foundry, the cristobalite formation should be maximized during the pouring process to aid shell knock-out process.

Therefore, if the preheating is integrated with the firing process as one step, a higher firing/preheating temperature (greater than 1000°C) should be used. It is noted that the shells needs to be kept at above 300°C before the hot metal is poured. This is to avoid the β to α transformation where micro cracking forms and weakens the shell.

However, if an investment foundry utilize a two-step heating before the final pour, i.e. firing-inspection-preheating, then a lower firing temperature (600°C) and a higher preheating temperature (1200°C) is preferred regarding to maximize the cristobalite formation during pouring. It is important to keep in mind that if one choose a lower firing temperature, additional layer of shell may be required to reach minimum shell strength.

The aluminum investment foundry will especially benefit from this research. Typically, the firing or preheating or pouring temperature in the aluminum investment foundry don't exceed the silica devitrification temperature. Therefore one can't take the advantages of cristobalite formation to aid the shell knock-out process. By utilizing suggested practices above, the shell knock-out process should be improved.

CONCLUSIONS AND FUTURE WORK

Colloidal silica binder was found to be the most active component within the ceramic shells with respect to devitrification during the multiple heating/cooling stages of investment casting processes. In this article, the effect of firing temperature on devitrification behavior of silica based shell molds was correlated with changes in thermal and mechanical properties.

Devitrification temperature range for this particular colloidal silica binder was found to start at around 1000°C (1832°F) at the heating rate of 15°C/min (27°F/min). For firing temperatures below 1000°C (1832°F), a higher firing temperature reduces the reactivity of the colloidal silica binder toward devitrification by decreasing specific surface area, resulting in less cristobalite formation upon reheating before mold pouring. The degree of devitrification affects the thermal conductivity of the shell molds. The excess heat generated from devitrification during the laser flash tests causes an underestimate of the heat capacity at 1200°C (2192°F).
Moreover, at below 1000°C (1832°F), increasing the firing temperature provides up to 40% more strength to the shell, whereas an even higher firing temperature (for example, 1200°C or 2192°F) decreases the shell strength by over 50% compared to the green shell.

It is noted that the firing time (one hour) used in this study is shorter than what a typical investment foundry uses. Therefore, the amount of devitrification which actually takes place may be much greater than the results presented in the paper. That will certainly magnify the effect of firing temperature on the thermo-physical properties. A proposal quantifying the kinetics of silica transformation at longer time has been approved by AFS 4L committee and AFS research board.

ACKNOWLEDGMENTS

The author wishes to thank Dr. Jeffery Smith for the helpful discussion. The author also would like to thank the graduate and undergraduate students in Materials Science and Engineering department at Missouri University of Science and Technology for their assistance.

REFERENCES

1. Beeley, P.R., Smart, R.F., Investment Casting, 1st ed., Institute of Materials (1995).
2. Jones, S., Yuan, C., Advances in shell moulding for investment casting, Journal of Materials Processing Technology 135 pp. 258–265(2003).
3. Venkat, Niranjan Das, Satyapal Singh, Sriramamuthy, A.M., "Defence Metallurgical Research Laboratory", Metals Materials and Processes, vol. 19, No. 1-4, pp. 203-224 (2007).
4. Doles, R.S., "A New Approach to the Characterization and optimization of Investment Casting Shell Systems", 9th world conference on investment casting: San Francisco, California, USA (1996).
5. Morrell, R., Quested, P.N., Jones, S., Ford, D.A., "Dimensional stability of ceramic casting moulds", NPL Report DEPC MPE (RES) 021.
6. Guerra, M., Schiefelbein, G.W., "Review of Shell Components, Shell Characteristics and Properties: Refractory Selection for Primary Shell Coat", Investment Casting Institute 42nd Annual Meeting, Atlanta, Georgia; USA; 25-28 (September 1994).
7. Austin, J.B., in Symposium. on Thermal Insulating Materials, Am. Soc. Testing Mater., Philadelphia, Pa., 1939, p. 3.
8. Francl, J., and Kingery, W.D., J. Am. Ceram. Soc., pp. 37-99 (1954).
9. Biancheria, A., Trans. Am. Nucl. Soc., 9 (1966) 15.
10. Aivazov, M.I. and Domashnev, I.A., Poroshkovaya Met., 8 (1968) 51.
11. Sugawara, Yoshizawa, Y., J. Appl. Phys., 33 (1962) 3135.
12. S.K. Rhee, "Porosity- Thermal conductivity Correlations for Ceramic Materials", Materials Science and Engineering, 20 (1975) 89-93.
13. Zivcova, Z., Gregorova, E., Pabst, W., Smith, D.S., Michot, A., Poulier, C., "Thermal conductivity of porous alumina ceramics prepared using starch as a pore-forming agent", Journal of the European Ceramic Society, 29 (2009) 347-353.
14. ASTM Standard, C1113, "Standard Test Method for Thermal Conductivity of Refractories by Hot Wire".
15. Heames, K., Geiger, G.H., "The Thermal Conductivity of Ceramic Shell Materials", Proceedings, 26th Annual Meeting of the Investment Casting Institute, 1973.

16. Huang, H., Berry, J. T., Zheng, X.Z., Piwonka, T.S., "Thermal conductivity of investment casting ceramics", 37th Annual Technical Meeting : Investment Casting Institute, Metal Casting Technology Center, University of Alabama.
17. Sabau, A.S., Viswanathan, S., "Thermo-physical properties of zircon and fused silica based shells for investment casting", AFS Transactions, vol. 112, pp. 649-661 (2004).
18. Shinzato, K., Baba, T., "A Laser Flash Apparatus for Thermal Diffusivity and Specific Heat Capacity Measurements", Journal of Thermal Analysis and Calorimetry, Vol. 64 (2001) 413–422.
19. ASTM E1461, "Standard Test Method for Thermal Diffusivity by the Laser Flash Method".
20. Connolly, S., Jones, S., Marquis, P.M., "Specific heat of investment casting shells," BICTA Issue 44, pp. 23-26 (2004).
21. Konrad, C.H., Brunner, M., Kyrgyzbaev, K., Völkl, R., Glatzel, U., "Determination of Heat Transfer Coefficient and Ceramic Mold Material Parameters for Alloy IN738LC Investment Castings", Journal of Materials Processing Technology 211 (2011) 181–186.
22. Garcia, E., Osendi, M.I., Miranzo, P., "Thermal diffusivity of porous cordierite ceramic burners," Journal of Applied Physics, volume 92, number 5, pp. 2346-2349 (2002).
23. Xu, M.; Lekakh, S.N.; Mahimkar, C.; Richards, V.L.; Dutler, S.A., "Measurements and Confirmation of Thermal Properties of Investment Ceramic Shell by Multiple Methods", Transactions of the American Foundry Society, Vol. 120, Paper No. 12-023, P 229-236, 2012
24. Xu, M.; Lekakh, S.N.; Richards, V.L., "An Improved Laser Flash Method to Determine Thermal Property of a Specimen with Porous Surfaces", submitted to Journal of Thermal Analysis and Calorimetry.
25. Hendricks, M.J., Engelhardt, D.R., "Thermal Conductivity and Heat transfer Measurement for Ceramic Shell Moulds", 8th World Conference on Investment Casting; Vol. 2, 1993.
26. Carlson, K.D., Beckermann, C., "Development of Thermo-physical Property Datasets, Benchmark Niyama Results, and A Simulation Qualification Procedure," Proceeding of the 64th SFSA Technical and Operating Conference, Paper No. 5.5 (2010).
27. Majchrzak, E., "Identification of Cast Steel Latent heat by Means of Gradient method," Int. J. Computational Materials Science and Surface Engineering, vol. 1, No. 5, pp.555-570 (2007).
28. Majchrzak, E., Dziewoński, M., Kałuża, G., "Numerical Algorithm of Cast Steel Latent Heat Identification", Journal of Achievements in Materials and Manufacturing Engineering, Vol. 22, Issue 1 (2007).
29. Hart, G., "The Nomenclature of Silica," American Mineralogist, vol. 12, pp. 383-395 (1927).
30. Mahimkar, C., Richards, V. L., Lekakh, S.N., "High Temperature Thermo-Physical Properties of Ceramic Shell," 57th Annual Technical Meeting: Investment Casting Institute (2010).
31. Meulenberg, W.A., Telle, R., Rothe, H., Sahm, P.R., "Fabrication and Investigation of Ceramic Shell Moulds for Investment Casting", Ceramic forum international; CFI; Berichte der DKG, vol 77-4 (2000).
32. ASTM C20, "Standard Test Methods for Apparent Porosity, Water Absorption, Apparent Specific Gravity, and Bulk Density of Burned Refractory Brick and Shapes by Boiling Water", ASTM International, 2000.
33. ASTM C1161, "Standard Test Method for Flexural Strength of Advanced Ceramics at Ambient Temperature", ASTM International, 2002.
34. Brunauer, S., Kantro, D. L., Weise, C. H., "The Surface Energies of Amorphous Silica and Hydrous Amorphous Silica", Canadian Journal of Chemistry, 1956, 34(10): 1483-1496, 10.1139/v56-190.
35. Beals, M.D., Zerfoss, S., "Volume Change Attending Low-To-High Inversion of Cristobalite," Journal of the American Ceramic Society, Volume 27, Issue 10, pages 285–292, November 1944
36. Kingery, W. D., Bowen, H. K., Uhlmann, D. R. (1975), Introduction to Ceramics. Cambridge, Massachusetts: Wiley